Vietnam Journal of Earth Sciences, 45(1), 49-66, https://doi.org/10.15625/2615-9783/17569

Vietnam Journal of Earth Sciences
https://vjs.ac.vn/index.php/jse

Establishment of the correlation between the near-surface sedimentary thickness and the microtremor dominant frequency in the Hanoi area

Hung Nguyen-Tien[1,2*], Phuong Nguyen-Hong[1,2*], Minh Nguyen-Le[1,2], Lin Che-Min[3], Nguyen Tran-An[1], Truyen Pham-The[1], Duong Nguyen-Van[1,2]

[1]*Institute of Geophysics, VAST, Hanoi, Vietnam*
[2]*Graduate University of Science and Technology, VAST, Hanoi, Vietnam*
[3]*National Center for Research on Earthquake Engineering (NCREE), Taiwan*

Received 26 June 2022; Received in revised form 29 August 2022; Accepted 10 October 2022

ABSTRACT

This paper established the correlation between the near-surface sedimentary thickness (D) and the microtremor dominant frequency (F_0) in the Hanoi area based on 64 microtremor measuring points at the boreholes with depth to bedrock. The microtremor dominant frequency was determined using the horizontal-to-vertical (H/V) spectral ratio of the seismic noise technique proposed by Nakamura (1989). The near-surface sedimentary thickness was determined according to the borehole data from the previously published reports. The non-linear regression method was applied to the pairs of D and F_0 values from 64 boreholes to obtain the relationship of form $D = 81.851*F_0^{-0.942}$. This correlation function was used to determine the values of the near-surface sedimentary thickness at microtremor measurement points according to the F_0 values. Comparison of the D-values obtained in this study with those from the boreholes data shows good coincidence by values and variation tendency, especially in areas with shallow cover thickness from 50 to 100 m. The above results allow the proposal of a new near-surface sedimentary thickness determination technique in the Hanoi area.

Keywords: near-surface sedimentary, microtremor, dominant frequency, correlation, Hanoi.

1. Introduction

Hanoi, the capital of Vietnam, is the political-administrative center of the country, with a population of approximately 8.5 million people. Hanoi is located in the Red River fault zone (RRF), stretching over 1000 km long in the northwest-southeast direction, as shown in Fig. 1. The RRF section that runs through Hanoi consists of 3 main faults: Red River fault, Chay River fault, and Lo River fault. Among them, the Chay River fault, which cuts through the center of Hanoi, is the most seismically dangerous. The estimated horizontal displacement speed along this fault at present is 2.7±1.6 mm/year (Phan

*Corresponding author, Email: ngtienhungvn@gmail.com, phuong.dongdat@gmail.com

et al., 2012; Phan et al., 2013). The Chay river fault is the leading cause of strong seismic shaking in the Hanoi area. Previous studies have shown that seismic intensity can reach level VIII (MSK-64 scale), making Hanoi a high seismic hazard area (Nguyen et al., 1994; Pham and Nguyen, 2019). In addition, Hanoi has many river systems flowing through, which have accreted a large amount of alluvial soil to create a large and flat plain. Therefore, Hanoi's shallow mantle is mainly composed of weak sediments lying parallel to the horizontal with a thickness of several tens of m. Ground motion in the surface layers is easily amplified by earthquake waves and can increase the damage.

- The investigations of strong earthquakes show that areas with thick near-surface soft soil layers are more destroyed and damaged than other areas (Lew, 1990; Singh et al., 1988; Fletcher and Wen, 2005). This is explained by amplifying the impacts of seismic waves' amplitude as they travel through this medium. Therefore, the near-surface sedimentary thickness is essential information in earthquake engineering practice. The near-surface sedimentary thickness is usually determined by several techniques such as engineering drilling (Vu et al., 2003; Bang and Kim, 2007), seismic exploration reflection/refraction methods (Hunter et al., 2002; Fkirin et al., 2016), multichannel analysis of surface waves (Miller et al., 1999; Ngal et al., 2019), etc. However, these techniques are often expensive and difficult to implement in densely populated areas, so they are often used only for specific construction sites.

- In recent years, the microtremor survey method has also been widely used to determine the near-surface sedimentary thickness due to its low cost, easy implementation in densely populated areas, and short survey time. This method measures the natural vibration signal on the ground by means of microtremor sensors without drilling or using a forced explosive source.

- Microseismic data are commonly used in the following techniques:

- Constructing the phase/group velocity curves using the microtremor data from array measurements (Capon, 1969; Tokeshi et al., 2006; Lin et al., 2009; Kuo et al., 2016). This technique allows for determining the near-surface sedimentary thickness and the wave velocity in that layer. Still, it requires a large enough survey area far from the noise sources. Therefore, it isn't easy to implement this method in densely populated or urban areas;

- Simulating the HVSR charts using the microtremor data from single-station microtremor data (Satoh et al., 2001a; Arai and Tokimatsu, 2005; Garcia-Jerez et al., 2007; Lin et al., 2014). This technique also allows us to determine the near-surface sedimentary thickness and the wave velocity in that layer. However, to assure high accuracy, the value of the shear-wave rate in the typical soil layers in the survey area should be known;

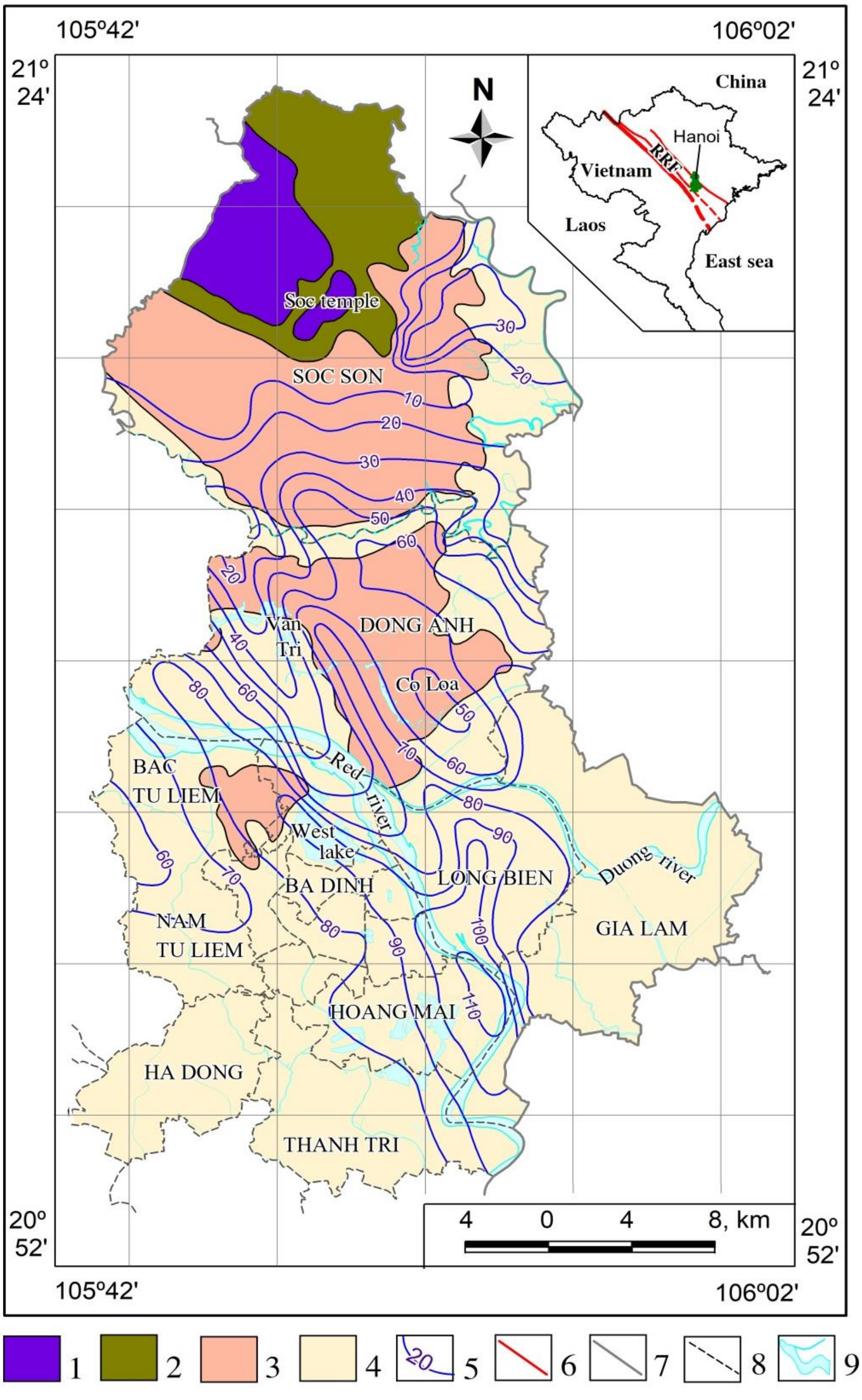

Figure 1. The study area's topography and near-surface sedimentary thickness map (after Nguyen et al.1996; Vu et al. 2003). (1) low mountain; (2) hilly areas; (3) high plain; (4) low plain; (5) contours of near-surface sedimentary thickness and value in meters (modified from Vu et al., 2003); (6) tectonic faults; (7) provincial boundary; (8) district boundary, and (9) rivers, lakes, or streams

- Constructing the empirical relationship between the near-surface sedimentary thickness and microtremor dominant frequency using data measured in the boreholes with depths reaching bedrock (Seht and Wohlenberg, 1999; Parolai et al., 2002; Dinesh et al., 2010; Gosar et al., 2010; Biswas et al., 2015; Abd et al., 2018; Molnar et al., 2018; Kumar and Mahajan, 2020; Tün and Pekkan, 2022). This technique is the easiest to implement but only allows for determining the parameters of the near-surface sedimentary thickness. In addition, to ensure the accuracy of the results, the survey area must have enough the number of boreholes with depths reaching bedrock.

Thus, it can be seen that each technique has its advantages and disadvantages. The appropriate survey technique should be chosen depending on the conditions and specific requirements.

In Vietnam, the microtremor survey method was first implemented by Soviet experts at the Hoa Binh hydropower plant in 1977 (Nguyen et al., 1990). The following studies can be mentioned, including Nguyen et al. (1994), Tuladhar et al. (2004); Tran et al. (2006); Nguyen et al. (2014). The common point of these studies is determining the dominant microtremor frequency/period for application in seismic microzonation or building 1D wave velocity structures. In contrast, other applications of the microtremor survey method are still limited. To expand the application research of microtremor, in this study, we present the results of establishing the empirical relationship between the dominant frequency of the microtremor vibration and the thickness of the near-surface sedimentary in the Hanoi area using supplemental data sources and propose a new technical procedure for determining the near-surface sedimentary thickness.

2. Geological engineering characteristics

- The survey area is about 1000 km^2, bounded in the range of latitude from 20^{o}52'N to 21^{o}24'N and longitude from 105^{o}42'E to 106^{o}02'E (see Fig. 1).

- According to the previously published reports, in the Hanoi area, the bedrock only outcrops in the northern mountainous area and then sinks under the near-surface sedimentary layer in the delta area (Nguyen et al., 1996; Vu et al., 2003). The Hanoi area is covered by a shallow Quaternary alluvial layer, formed from the Early Pleistocene to the Late Holocene, which includes 5 formations from top to bottom, namely Thai Binh, Hai Hung, Vinh Phuc, Hanoi, and Le Chi, respectively. The main composition of this near-surface sedimentary layer is fine-grained sand, clay, yellow sand, gravel, and pebbles (Figs. 2, 3).

- Vu et al. (2003) show that the near-surface sedimentary thickness tends to increase gradually from north to south (reaching 0 m in Soc Son district and 116 m in Hoang Mai district) as well as from west to east (reaching 55 m in Bac Tu Liem district and 100 m in Long Bien district). The near-surface sedimentary thickness along the Red River bank increases rapidly, creating a stiffer near-surface of a valley form, stretching in a northwest-southeast direction from Dong Anh district to Hoang Mai district and covering the entire Long Bien district. The near-surface sedimentary thickness in southern districts (Thanh Xuan, Ha Dong, Thanh Tri) and the Gia Lam district has stable values (from 70 to 80 m). The near-surface sedimentary thickness in the southern part of Soc Son district (from 10 to 50 m) and the west of Dong Anh district (from 40 to 80 m) tends to change rapidly, creating a hard rock surface inclined to the south (Figs. 1, 3).

Period	Epoch	Formation	Symbol	Lithology	Thickness (m) Set	Thickness (m) Total	Description
QUATERNARY	HOLOCENE	THAI BINH	$aQ_{IV}^{3}tb_2$		2-5	15	Set 2: silty clays containing snails, mussel, humus
					3-10		Set 1: fine-grained sand with silty clay
			$aQ_{IV}^{3}tb_1$		1-5	31	Set 3: Clayey silt interbedded with humus
					3-18		Set 2: silty sand interbedded with humus
					1-9		Set 1: gravel with sand, coarse-grained sand
		HAI HUNG	$bQ_{IV}^{12}hh$		2	12	Swamp sediments: Mud, silty clay containing peat
			$mQ_{IV}^{12}hh_2$		1-9		Sea sediments: Clay, silty clay
			$lbQ_{IV}^{12}hh_1$		2-6		Lake-swamp sedimemts: Silty clay with plant remains, peat
	PLEISTOCENE	VINH PHUC	$lbQ_{III}^{2}vp_3$		3-8	61	Set 4: Silty clay, black clay (lake-swamp accumulation)
			$lQ_{III}^{2}vp_2$		10		Set 3: Kaolin clay, grey silty clay
			$aQ_{III}^{2}vp_1$		33		Set 2: Sand mixed with clay, yellow building sand
					10		Set 1: Pebbles, gravel, sand, silty clay
		HA NOI	$ap, aQ_{II-III}^{1}hn$		4	55	Set 3: Silty clay with plant remains
					17		Set 2: Silty sand, coarse-grained sand, gravel
					34		Set 1: Cobbles, conglomerate, gravel, silty sand
		LE CHI	$aQ_{I}^{1}lc$		1-3	25	Set 3: Clayey silt, grey sand
					2-5		Set 2: Silty sand, small grained sand
					20		Set 1: cobbles, gravel, clayey silt

Figure 2. Stratigraphic column for the Quaternary of the Hanoi area (modified from Dai et al., 1996)

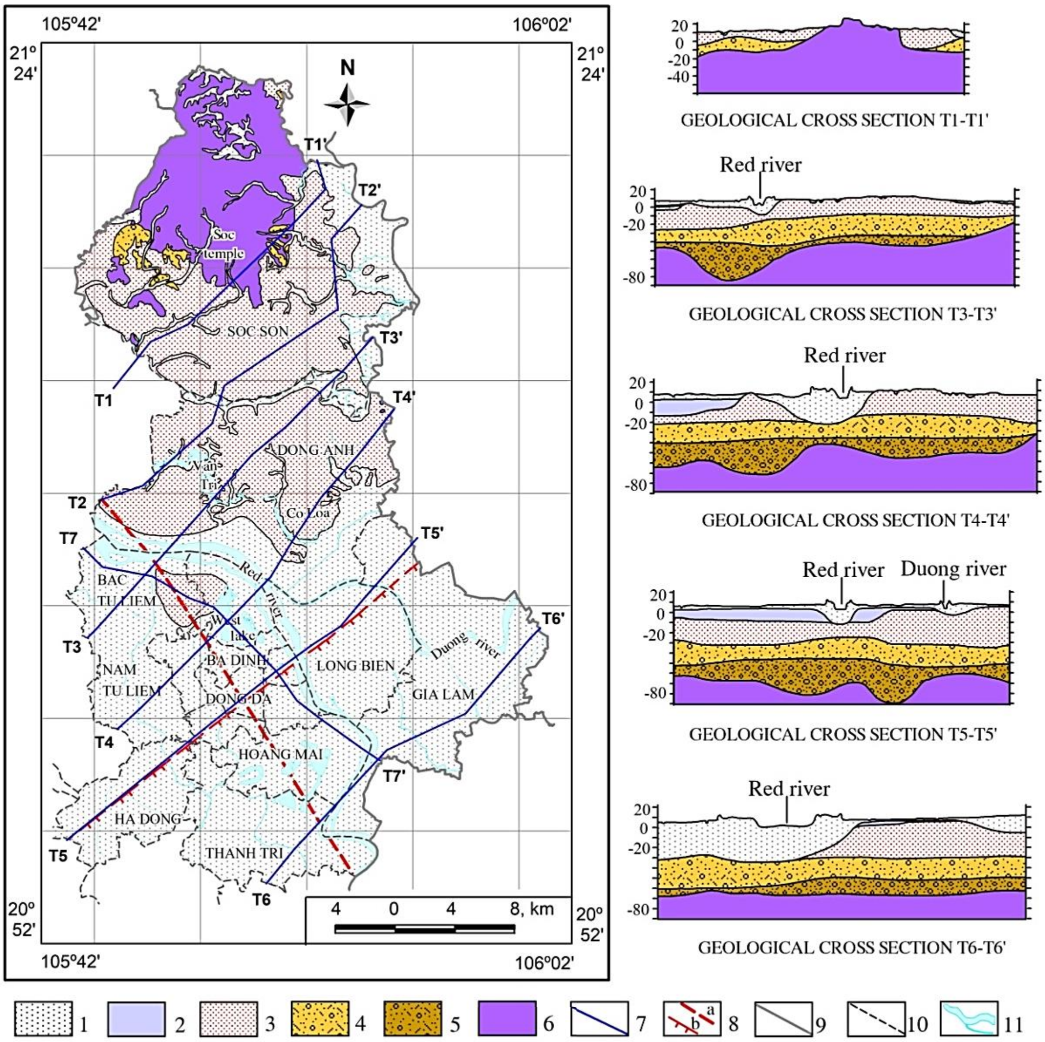

Figure 3. Engineering geological zoning map and the 2-D geological cross-sections of the Hanoi area. (1) Thai Binh formation; (2) Hai Hung formation; (3) Vinh Phuc formation; (4) Ha Noi formation; (5) Le Chi formation; (6) hard rock; (7) geological cross-section; (8) tectonic fault, a - Vinh Ninh fault, b - Gia Lam-Chuong My fault; (9) provincial boundaries; (10) district boundaries and (11) river, stream, or lake (modified from Nguyen et al., 1996)

3. Data and Method

3.1. Data

The data used in this study include:

- 834 single-station microtremor measurement points, of which 67 measurement points next to the borehole with depth to bedrock and 258 measurement points along the survey profiles (7 profiles coincide with the geological cross-section by Nguyen et al. (1996) and 2 profiles in the north-south and east-west directions) (Fig. 4). The equipment used is a microtremor measuring device manufactured by Tokyo Sukushin, Japan. Each set includes a SAMTAC-801H recorder and a VSE315D or VSE355EV sensor. The recorder has a 24bit resolution, and the sensor has 6 components (3 velocity components and 3 acceleration components) with a frequency range from 0.1 to 50 Hz. At each point, measurements were made continuously over 20 minutes. The sampling frequency of the measurement is 200 samples/second. The data used for analysis are microtremor vibration tapes' three velocity components (NS, EW, Z). Measurement points are precisely located using a handheld global positioning system (GPS). The dominant frequency of micro-tremor vibration (F_0) was determined by Nakamura's H/V spectral ratio analysis technique (1989).

- 113 geological engineering boreholes, of which 88 have a depth to bedrock (Nguyen et al., 1996; Vu et al., 2003; Nguyen et al., 2012).

- 7 geological engineering cross-sections by Nguyen et al. (1996), of which 6 cross-sections are in the northeast-southwest direction and one in the northwest-southeast direction. Based on these 7 cross-sections, we have established 7 structural cross-sections of the near-surface sedimentary thickness (thickness of the Quaternary sediments). However, from 1996 to the present, some of these structural cross-sections have been studied in more detail by the new boreholes data (Vu et al., 2003; Nguyen et al., 2012), so we performed to evaluate the reliability of these structural cross-sections. Update this near-surface sedimentary thickness was determined according to the new borehole data (solid green circle) on these structural cross-sections (Fig. 5). Figure 5 shows that most of the near-surface sedimentary thickness was determined according to the new borehole data and the structural cross-sections of Nguyen et al. (1996) are significantly different. It proves that the near-surface sedimentary thickness determined according to the structural cross-sections of Nguyen et al. (1996) is still not true to reality. Therefore, previous studies determined the near-surface sedimentary thickness according to the borehole data.

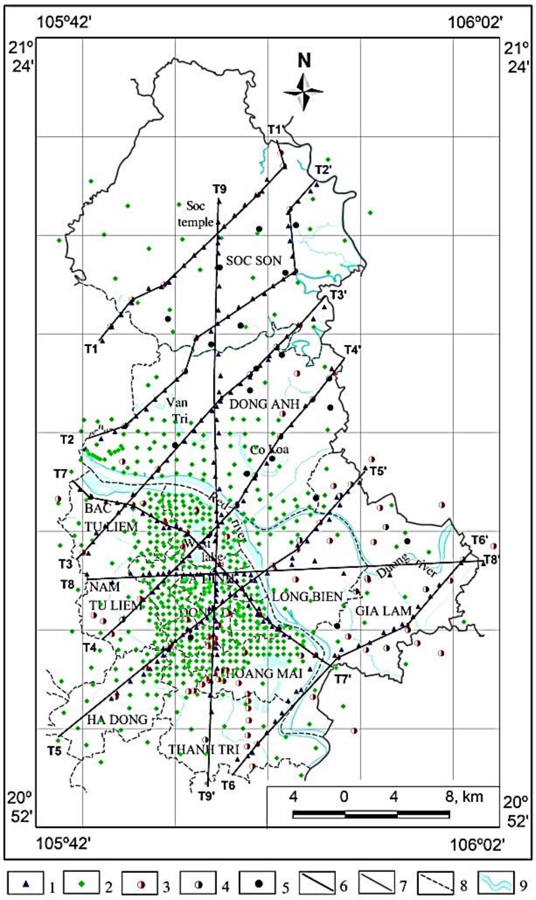

Figure 4. This study uses a map of the distribution of single-station microtremor measurement points and geological boreholes. (1) microtremor measurement points along profiles; (2) area microtremor measurement points; (3) boreholes with depth to bedrock; (4) other boreholes; (5) vertical electrical sounding stations; (6) microtremor survey profiles; (7) provincial boundary; (8) district boundary and (9) rivers, lakes, or streams

The measurement error is determined as follows:

$$\text{Err} = \frac{|\bar{A}-A_n|}{\bar{A}} * 100\ (\%) \qquad (1)$$

where n is the number of measurements, A_n is the n^{th} measurement value, $\bar{A}$ is the average value of n measurements, determined as follows:

$$\bar{A} = \frac{A_1+A_2+\cdots+A_n}{n} \qquad (2)$$

Formula (1) was used to calculate the F_0 error for the microtremor data of the previous study (Hung et al., 2017). The average error of F_0 calculated for 49 loop measurements and 84 simultaneous measurements at 12 points using 7 Samtac apparatus were 2.9% and 1.5%, respectively (see Fig. 6). As shown in Fig. 6, 44 of the 49 loop measurements and 79 of 84 simultaneous measurements had the error of F_0 not exceeding 5%. The largest F_0 error is 11.1% observed at the A7 measuring point (in the Long Bien district), corresponding to the area with a depth greater than 90 m depicted in Fig. 1.

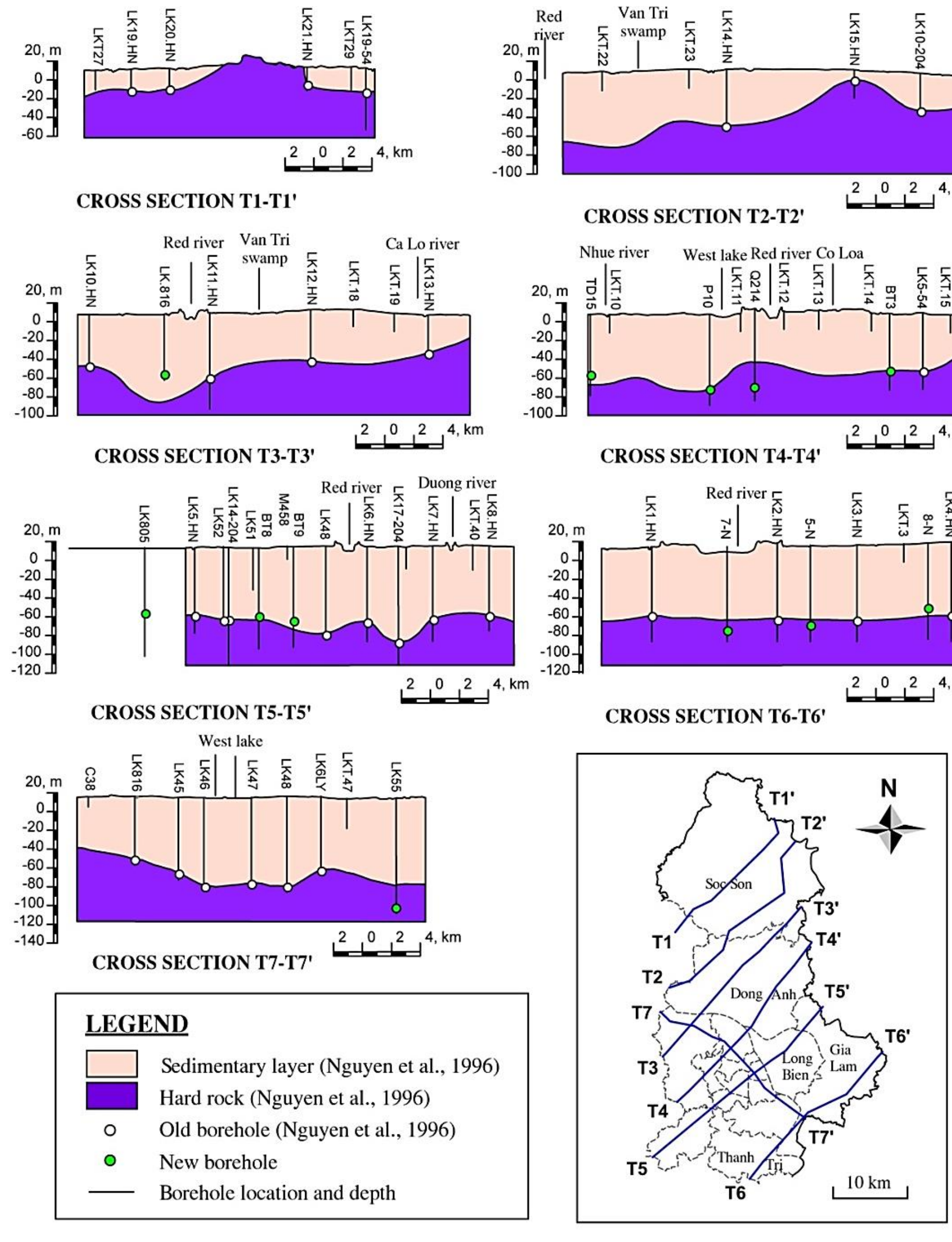

Figure 5. The structural cross-sections of the near-surface sedimentary thickness and borehole locations in the Hanoi area

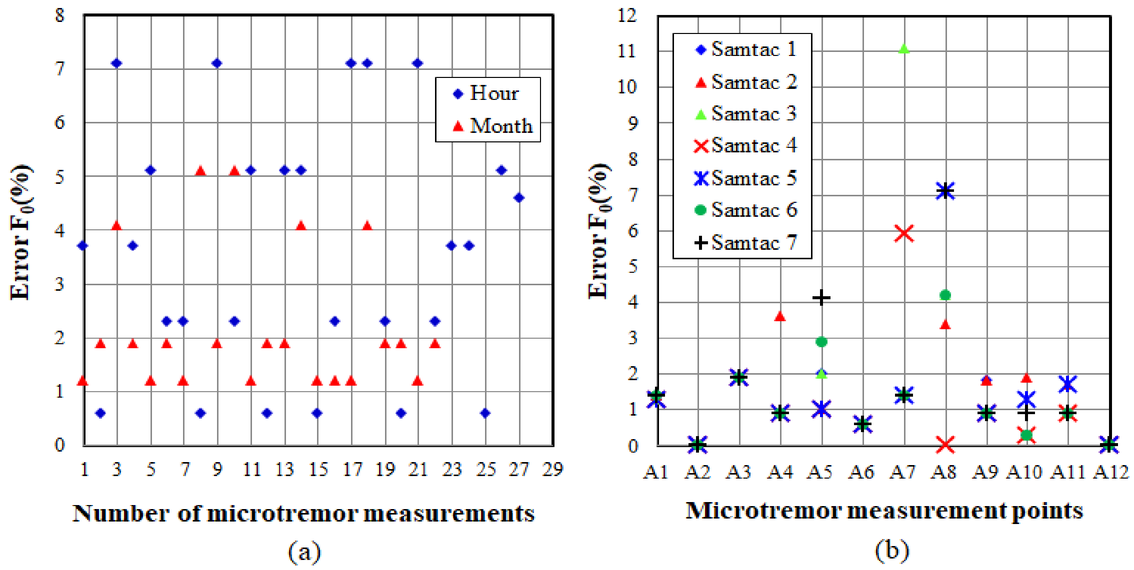

Figure 6. The F_0 error chart of microtremor measurement. (a) 49 loop measurements over time and (b) 12 simultaneous measurement points by 7 Samtac seismometers

3.2. Method of the establishment of the correlation between the near-surface sedimentary thickness and the microtremor dominant frequency

Seht and Wohlenberg proposed this method in 1999. The theoretical correlation was established for a simple two-layer model as shown in Fig. 7: a hard rock basement is covered by a soft soil layer of thickness D and shear-wave velocity V_S.

According to this model, the transfer function has maxima at frequencies:

$$F_0 = \frac{n.V_S}{4D} \quad (n = 1, 3, 5, \ldots) \tag{3}$$

A velocity-depth function in a soft soil layer is of the form:

$$V_S(z) = V_0.(1+Z)^x \tag{4}$$

where V_0 is the surface shear-wave velocity, Z = z/z_0 (with z_0 = 1 m), and x gives the depth dependence of the velocity. The value of *x* is obtained empirically.

As by definition, V(z)=dz/dt, the travel time in the soft soil layer (layer 1) is calculated as

$$t = \int_0^D \frac{dz}{V_S(z)} = \frac{1}{V_0}\int_0^D (1+Z)^{-x} dz = \frac{1}{V_0}\frac{(1+D)^{1-x}-1}{(1-x)} \tag{5}$$

On the other hand, the relation between F_0 and t is defined by:

$$F_0 = \frac{1}{4t} = \frac{V_0(1-x)}{4[(1+D)^{1-x}-1]} \tag{6}$$

where F_0 is in Hz, V_0 is in m/s, and D is in m. From (6) we have:

$$D + 1 = \left[\frac{V_0(1-x)}{4F_0} + 1\right]^{1/(1-x)} \tag{7}$$

Empirically proven that D >> 1 => D + 1 ≈ D; $\frac{V_0(1-x)}{4F_0} \gg 1 \Rightarrow \frac{V_0(1-x)}{4F_0} + 1 \approx \frac{V_0(1-x)}{4F_0}$

Therefore, equation (7) can be written in a more simple form:

$$D = a * F_0^b \tag{8}$$

where $a = \left[\frac{V_0(1-x)}{4}\right]^{1/(1-x)}$; $b = -\frac{1}{1-x}$ and are depending on the local ground conditions.

The method was applied to the western zone of the Lower Rhine Embayment (Germany) based on 34 microtremor measuring points in boreholes and found a related equation of the form $D = 96 * F_0^{-1.388}$. Up to now, this approach has been successfully applied in many parts of the World (Abd et al., 2018; Biswas et al., 2015; Gosar and Lenart, 2009; Milkereit et al., 2002).

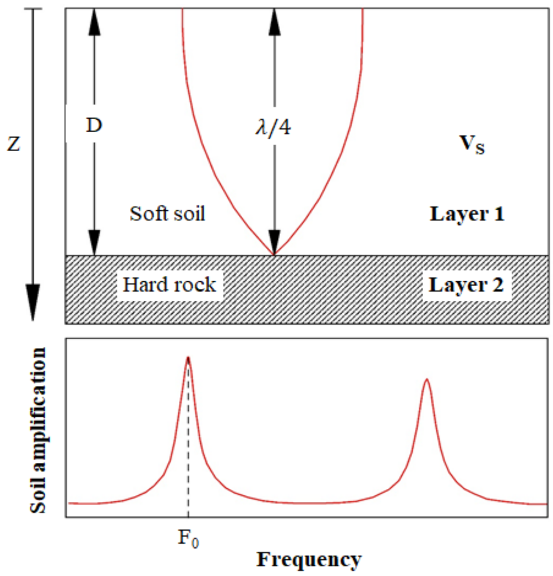

Figure 7. The two-layer model proposed by Seht and Wohlenberg (1999) includes a hard rock basement covered by a soft soil layer

3.3. Data analysis

The data analysis process includes the following steps:

- Step 1: Determine the parameters of formula (8), including 1- the values of the actual near-surface sedimentary thickness (D_K) at 67 boreholes along the survey profiles provided by Nguyen et al. (1996); Vu et al. (2003) and Nguyen et al. (2012); 2- the values of the microtremor dominant frequency (F_0) measured at 67 points coincide with the boreholes mentioned above.

- Step 2: Determine the coefficients a and b of formula (8) according to the non-linear regression of the form $D_K = a * F_0^b$.

- Step 3: Evaluate errors of the near-surface sedimentary thickness.

- Step 4: Deduce the near-surface sedimentary thickness in the remaining microtremor measurement points according to the above correlation function;

- Step 5: Compare the results of this study with the previously published results.

4. Results

The Nakamura technique (1989) was applied to 834 single-station microtremor measurement points to obtain 831 corresponding F_0 values. From 67 pairs of D_K and F_0 values obtained, 64 reliable pairs we selected (Table 1). Using non-linear regression for the function of the form $D_K = a * F_0^b$ of these 64 pairs of D_K and F_0 values, we found the values of the coefficients, namely a = 81.851; b = -0.942, with a correlation coefficient of 0.84 (Fig. 8).

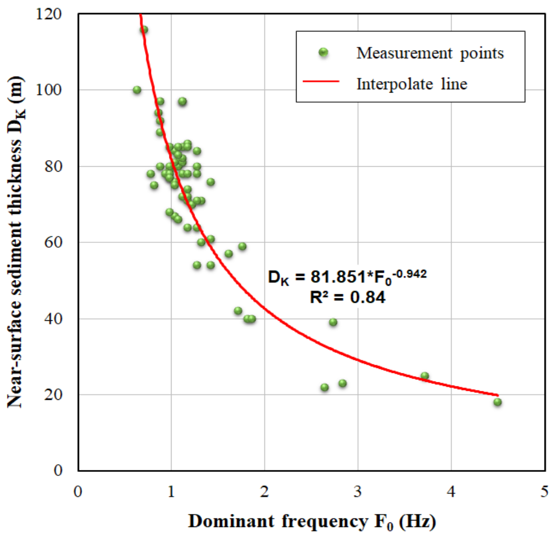

Figure 8. The empirical correlation between the near-surface sedimentary thickness (D_K) and microtremor dominant frequency (F_0) in the Hanoi area

So the empirical correlation equation between D_K and F_0 in the Hanoi area has the form:

$$D_K = 81.851 * F_0^{-0.942} \qquad (9)$$

The correlation coefficient obtained for formula (9) shows the high correlation between D_K and F_0 values in the Hanoi area. Therefore, formula (9) was applied to determine the near-surface sedimentary thickness according to the value F_0 at all single-station microtremor measurement points in this study. Formula (1) was used to calculate errors of the near-surface sedimentary thickness for 64 pairs of D_T and D_K values (Err. in Table 1).

From 258 values of D_T and D_K on 9 measurement profiles illustrated in Fig. 4, 9 cross-sections were created showing the near-surface sedimentary thickness along the measurement profiles (Fig. 9). Finally, the interpolation method is applied to 831 D_T values to develop the Hanoi area's near-surface sedimentary thickness zoning map (Fig. 10).

Table 1. Summary of the data used and the results obtained in this study

N^0	Measuring point	Borehole	F_0 (Hz)	D_K (m)	D_T (m)	Err (%)	Notes
1	T116	LK21.HN	4.49	18	20	10	(1)
2	T106	LK20.HN	2.64	22	33	49	(1)
3	T104	LK19.HN	2.83	23	31	34	(1)
4	T119	LK19-54	3.71	25	24	5	(1)
5	T225	LK10-204	2.73	39	32	19	(1)
6	132	Q213	1.71	42	49	18	(3)
7	T428	LK9-204	1.86	40	46	14	(1)
8	T326	LK13.HN	1.81	40	47	17	(1)
9	T301	LK10.HN	1.27	54	65	21	(1)
10	T317	LK12.HN	1.42	54	59	9	(1)
11	969	BT1	1.61	57	52	8	(2)
12	T212	LK14.HN	1.76	59	48	19	(1)
13	T424	BT3	1.32	60	63	5	(2)
14	T426	LK5-54	1.42	61	59	4	(1)
15	T306	LK.816	1.17	64	71	10	(1)
16	T401	TD15	1.27	64	65	2	(3)
17	740	LĐ2	1.07	66	77	16	(3)
18	T309	LK11.HN	1.03	67	80	19	(1)
19	175	CĐ10	0.98	68	83	23	(3)
20	T622	8-N	1.22	70	68	3	(3)
21	T504	805	1.17	71	71	0	(3)
22	T508	LK5.HN	1.32	71	63	11	(1)
23	T940	LĐ4	1.27	71	65	8	(3)
24	T516	BT8	1.17	72	71	2	(2)
25	T604	LK1.HN	1.12	72	74	2	(1)
26	555	ĐC4	1.17	74	71	5	(3)
27	T726	LK6LY	0.81	75	100	33	(1)
28	706	LĐ5	1.03	75	80	6	(3)
29	T513	LK.14-204	1.03	76	80	5	(1)
30	412	BT7	1.42	76	59	23	(2)
31	T624	LK4.HN	0.98	77	83	8	(1)
32	781	PV2	0.98	77	83	8	(3)
33	T520	BT9	1.27	78	65	16	(2)
34	T538	LK8.HN	0.93	78	88	12	(1)
35	T618	LK3.HN	1.12	78	74	6	(1)
36	T710	LK45	0.98	78	83	7	(1)
37	587	ĐC3	1.17	78	71	9	(3)
38	924	BT6	0.78	78	103	33	(2)
39	T410	P10	0.98	79	83	6	(3)
40	T527	LK6.HN	0.88	80	92	15	(1)
41	588	ĐC1	1.07	80	77	4	(3)
42	707	LĐ6	1.27	80	65	18	(3)
43	663	4-63	0.98	80	83	4	(3)
44	T937	ĐC2	1.12	81	74	9	(3)

N^0	Measuring point	Borehole	F_0 (Hz)	D_K (m)	D_T (m)	Err (%)	Notes
45	T938	BT10	1.07	81	77	5	(2)
46	61	BT4	1.07	81	77	5	(2)
47	726	LĐ3	1.03	81	80	2	(3)
48	T935	ĐC5	1.12	82	74	10	(3)
49	739	LĐ1	1.07	83	77	7	(3)
50	T414	Q214	1.03	84	80	5	(3)
51	518	P44	1.27	84	65	22	(3)
52	T934	Q215	1.17	85	71	17	(3)
53	655	BT11	1.12	85	74	13	(2)
55	741	LĐ7	1.07	85	77	10	(3)
55	729	LĐ8	0.98	85	83	2	(3)
56	T615	5-N	1.17	86	71	18	(3)
57	T716	LK47	0.88	89	92	4	(1)
58	T714	LK46	0.88	92	92	0	(1)
59	T524	LK48	0.86	94	94	0	(1)
60	T539	9-63	1.12	97	74	24	(3)
61	766	7-N	0.88	97	92	5	(3)
62	915	9-63	1.12	97	74	24	(3)
63	T530	LK.17-204	0.63	100	126	26	(1)
64	T736	LK55	0.70	116	115	1	(1)

Note: F_0: Microtremor dominant frequency; D_K: The near-surface sedimentary thickness obtained from the borehole data; D_T: The near-surface sedimentary thickness obtained from microtremor data; Err: The near-surface sedimentary thickness error; (1) According to Nguyen et al. (1996); (2) According to Vu et al. (2003); (3) According to Nguyen et al. (2012)

5. Discussions

As shown in Table 1, 38 of 64 pairs of D_T and D_K values have errors less than 10%, 15 of 64 pairs of values D_T and D_K have errors in the range of 10%-20%, and 11 of 64 pairs of values D_T and D_K have an error greater than 20%. These results show a good correlation between the near-surface sedimentary thickness obtained by this study and measured in the boreholes. The best correlation is observed in the depth range from 50 to 100 m (corresponding to the southern area, Dong Anh district, along the Red River bank, and the south zone of Gia Lam district). In contrast, the worst correlation is observed in the depth range of less than 25 m (corresponding to the mountainous or the mountain foot delta of Soc Son district).

Figure 8 also shows a good correlation between the established empirical equation (the interpolated dark red curve) with the data (solid green circle). However, a significant deviation is observed at the two points corresponding to the near-surface sedimentary thickness of about 20 m. This suggests that equation (9) is not yet suitable for this thickness.

Figure 9 shows a good coincidence between most of the D_T values (the blue diamonds) at the boreholes and D_K values (Nguyen et al., 1996; Vu et al., 2003; Nguyen et al., 2012, the solid green circles). As seen in Table 1, 42 of 47 boreholes have less than 25% thickness errors. The most significant difference can only be observed at three boreholes, namely the LK15.HN borehole at measuring point 21 on the T2-T2' profile; the LK7.HN borehole at measuring point 32 on the T5-T5'profile and the LK6LY borehole at measuring point 26 on the T7-T7' profile. This difference can be explained by different techniques used to determine thickness. The D_K value obtained from the boreholes is determined based on lithological characteristics. It is not affected by rock-soil layers' moisture, compaction, and water saturation.

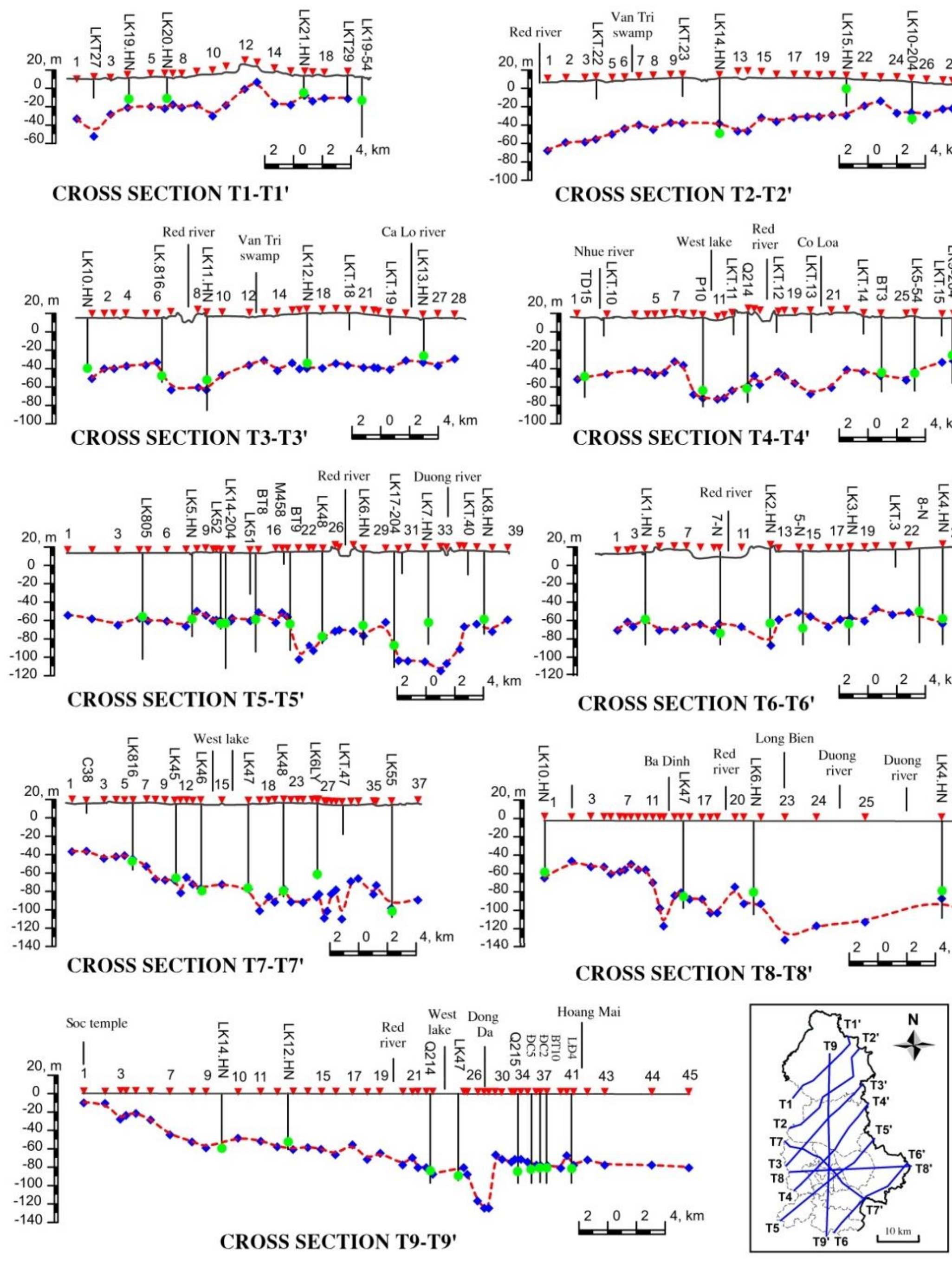

Figure 9. Distribution of the near-surface sedimentary thickness along 9 cross-sections. The red triangles above are the location of the microtremor measurement points; The blue diamonds are the thickness values obtained by formula (9); The solid green circles are the thickness values obtained by boreholes; The vertical black lines are the borehole positions with their respective depths; The red dashed lines are the boundary between the near-surface sedimentary layer and bedrock determined by this study. The microtremor measurement points' names and the boreholes' names are described above the cross-sections

In contrast, in this study, the D_T values are obtained mainly by the average shear-wave velocity, which is affected by rock-soil layers' moisture, compaction, and water saturation. Therefore, the difference here may be due to the influence of saturated water content in strongly weathered of rock-soil layers (above solid rock). This rock layer will reduce the V_S value leading to F_0 amplification by the deeper hard rock layer. The field survey at the LK15.HN borehole shows that the exposed rock is high to moderately weathered rock. The calculation of the D_T value at the LK15.HN borehole (D_K reaches 11 m, the thin near-surface sedimentary thickness) by formula (9) can also cause differences because this formula is not yet suitable for the area with the thin near-surface sedimentary thickness. At the LK7.HN borehole (D_K reaches 77 m) and LK6LY borehole (D_K reaches 75 m), the difference may also be due to the influence of the seismometer error (measurement point A7, reaching 11.1%, Fig. 6). Therefore, to clarify this discrepancy, it is necessary to carry out other survey techniques, especially the borehole seismic measurement techniques.

Although there are still differences in some boreholes, an overall look at the cross-sections reveals a clear correlation between the topographic surface (solid black lines above) and the hard rock surface identified in this study (red dashed lines below). Thus, in the raised terrain surface (hilly areas), the section from the 11 to 14 measurement points on the T1-T1' profile, the corresponding hard rock surface also rises. In contrast, when the terrain surface is depression down (in the river-lake areas), as shown in the sections from the 6 to 10 measurement points on the T3-T3' profile, from the 8 to 22 measurement points on the T4-T4' profile and the 25 to 28 measurement points on the T5-T5' profile, the corresponding hard rock surface also depresses down. The T4-T4' survey profile, which crosses the West Lake, Red River, and Co Loa, shows that the West Lake area has the thickest cover layer (over 100 m), which tends to tilt (about 70^o) northeastward, bounding the small Red river depression in the middle and adjacent to the large Co Loa depression.

As seen in Fig. 10, the variation of the D_T is consistent in trend and values with the D_K (Vu et al., 2003, Fig. 1). The near-surface sedimentary thickness tends to increase gradually from north to south (less than 20 m in Soc Son district and more than 110 m in Hoang Mai district) and from west to east (less than 60 m in Bac Tu Liem district and more than 100 m in Long Bien district). The layer depth along the Red River banks is increasing rapidly, with a hard rock surface in the valley form, in a northwest-southeast direction, extending from Dong Anh district to Hoang Mai district and extending to the end of Long Bien district. The near-surface sedimentary thickness is stable (from 70 to 80 m) in the southern districts (Thanh Xuan, Ha Dong, Thanh Tri). However, D_T and D_K values are still different at some structural boundaries. According to Vu et al. (2003), the D_K values have a gradual change, but according to this study, the D_T values change occurs abruptly. This might be due to the considerable increase in this study's measuring points. The high density of microtremor data in this study allows us to determine the position and shape of the hard rock surface at some structural boundaries. Thus, the sedimentary layer located southwestward of the Red River strip has a steep wall form (from 60 to 80 m), inclined to the northeast (about 70^o, see Fig. 9), very near the location of the Vinh Ninh fault (blue dashed line). In this study, the thickness of the sedimentary layer in the northern mountainous zone changes rapidly (from 20 to 40 m), inclined to the south (about 30^o) at the mountain foot, and then gradually changes in the delta areas. The Co Loa zone has a valley form with a northwest-southeast direction inclined to the southeast. According to Vu et al. (2003) (determined by vertical electrical sounding data), this is a ridge. A comparison of the actual topography in this zone shows that the river and lake system has the shape of horseshoes, which proves that this is a depression zone. Therefore, the results of this study are more consistent with reality.

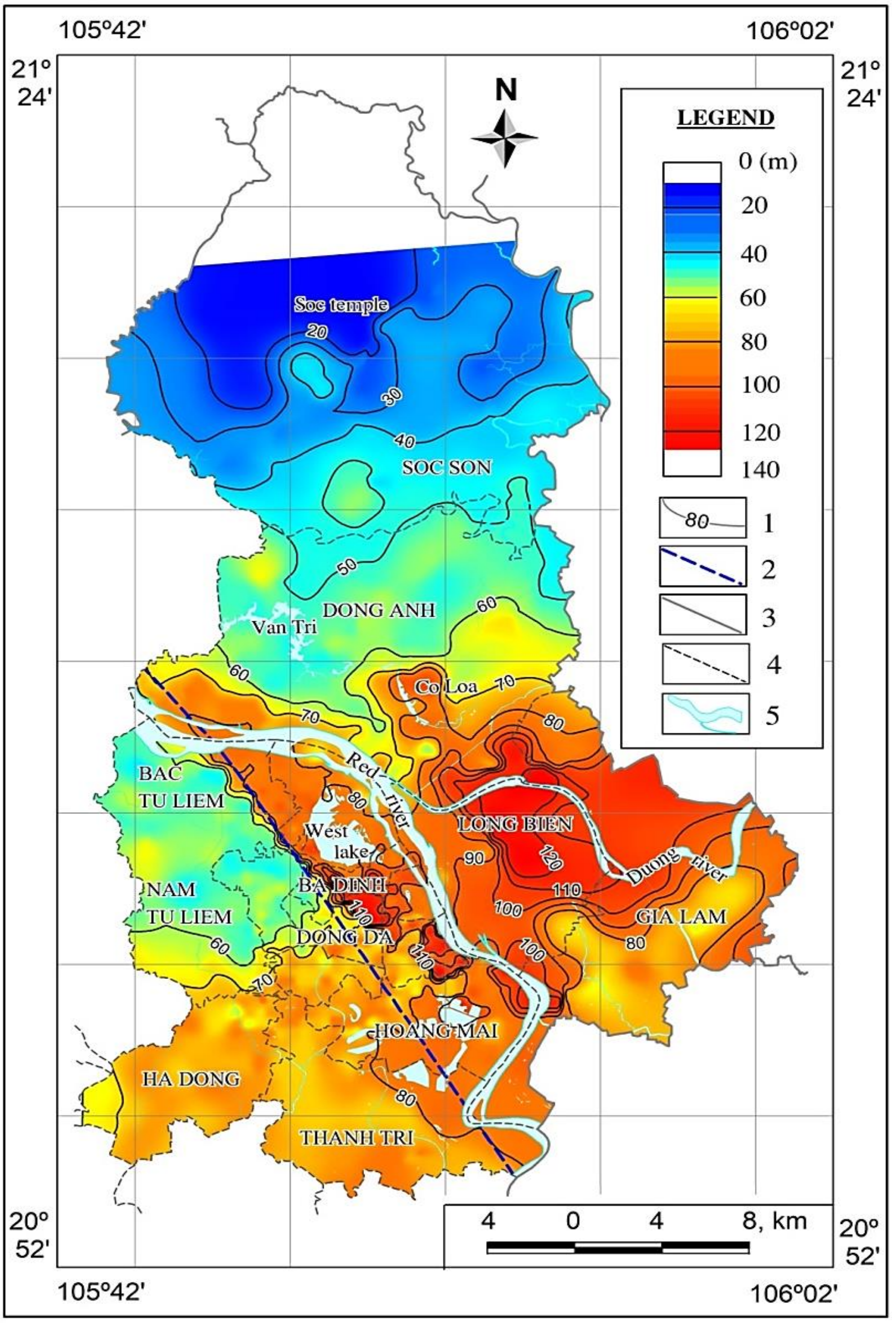

Figure 10. Distribution of the near-surface sedimentary thickness in the Hanoi area obtained from microtremor data. (1) the near-surface sedimentary thickness and value in meter; (2) tectonic fault; (3) provincial boundaries; (4) district boundaries and (5) river, stream, or lake

6. Conclusions

This study used microtremor data to establish the correlation between the near-surface sedimentary thickness and the microtremor dominant frequency in the Hanoi area. A total of 64 microtremor measurement points were carried out next to the boreholes. Based on the analysis of the results, some conclusions can be drawn as follows:

- The empirical relationship function between the near-surface sedimentary thickness D (in m) and the microtremor dominant frequency F_0 (in Hz) established for the Hanoi area has the form:

$$D = 81.851*F_0^{-0.942}.$$

- The near-surface sedimentary thickness error reached less than 10% in the southern zone, Dong Anh district, along the Red River bank, and the southern zone of Gia Lam district, corresponding to the near-surface sedimentary thickness from 50 to 100 m, and the largest reached over 30% in the mountainous or the mountain foot delta of Soc Son district, corresponding to the near-surface sedimentary thickness less than 25 m.

- The near-surface sedimentary thickness obtained by the microtremor data is consistent with the boreholes data distributed by profiles and area. The near-surface sedimentary thickness reaches less than 20 m in the northern mountains of the Soc Son district and over 100 m in the central and eastern areas. The near-surface sedimentary thickness of the strip along the Red River bank and the southern area reached over 70 m.

Acknowledgments

This study has been funded by the Vietnam Academy of Science and Technology (VAST) under grant number: CSCL12.02/22-22. Hung Nguyen-Tien was supported by the Graduate University of Science and Technology (GUST) for his Ph.D. study.

References

Abd E-A., Khairy, Abd E-A., 2018. New relationship between fundamental site frequency and thickness of soft sediments from seismic ambient noise. J. Seismol., 22, 1315-1323.

Arai H., Tokimatsu K., 2005. S-Wave Velocity Profiling by Joint Inversion of Microtremor Dispersion Curve and Horizontal-to-Vertical (H/V) Spectrum. Bulletin of the Seismological Society of America, 95(5), 1766-1778.

Bang E.S., Kim D.S., 2007. Evaluation shear wave velocity profile using SPT based uphole method. Soil Dynamics and Earthquake Engineering, 27(8), 741-758.

Biswas R., Baruah S., Bora D.K., 2015. Mapping Sediment Thickness in Shillong City of Northeast India through Empirical Relationship. Journal of Earthquakes. https://doi.org/10.1155/2015/572619.

Capon J., 1969. High-resolution frequency-wavenumber spectrum analysis. Proceedings of the IEEE, 57(8), 1408-1418.

Dinesh B.V., Nair G.J., Prasad A.G.V., Nakkeeran P.V., Radhakrishna M.C., 2010. Estimation of sedimentary layer shear wave velocity using micro-tremor H/V ratio measurements for Bangalore city. Soil Dynamics and Earthquake Engineering, 30, 1377-1382.

Fkirin M.A., Badawy S., El deery M.F., 2016. Seismic Refraction Method to Study Subsoil Structure. J. Geol. Geophys., 5(5), 1-6.

Fletcher J.B., Wen K.L., 2005. Strong Ground Motion in the Taipei Basin from the 1999 Chi-Chi, Taiwan, Earthquake. Bulletin of the Seismological Society of America, 95(4), 1428-1446.

Garcia-Jerez A., Navarro M., Alcala F.J., Luzon F., Perez-Ruiz J.A., Enomoto T., Vidal F., Ocana E., 2007. Shallow velocity structure using joint inversion of array and h/v spectral ratio of ambient noise: The case of Mula town (SE of Spain). Soil Dynamics and Earthquake Engineering, 27, 907-919.

Gosar A., Lenart A., 2010. Mapping the thickness of sediments in the Ljubljana Moor basin (Slovenia) using microtremors. Bull Earthquake Eng., 8, 501-518.

Hung Nguyen-Tien, Phuong Nguyen-Hong, Minh Nguyen-Le, Wen Kuo-Liang, Nguyen Tran-An, 2017. Investigation of microtremor motion variation by Nakamura's H/V spectral ratio method. Journal of Marine Science and Technology, 17(4B), 68-74. Doi: 10.15625/1859-3097/17/4B/12994.

Hunter J.A., Benjumea G., Harris J.B., Miller R.D., Pullan S.E., Burns R.A., Good R.L., 2002. Surface and downhole shear wave seismic methods for thick soil site investigations. Soil Dynamics and Earthquake Engineering, 22, 931-941.

Kumar P., Mahajan A.K., 2020. New empirical relationship between resonance frequency and thickness of sediment using ambient noise measurements and joint-ft-inversion of the Rayleigh wave dispersion curve for Kangra Valley (NW Himalaya), India. Environmental Earth Sciences, 79(256), 1-14.

Kuo C.K., Chen C.T., Lin C.M., Wen K.L., Huang J.Y., 2016. S-wave velocity structure and site effect parameters derived from microtremor arrays in the Western Plain of Taiwan. Journal of Asian Earth Sciences, 128, 27-41.

Lew H.S., 1990. Performance of Structures During the Loma Prieta Earthquake of October 17, 1989. National Institute of Standards and Technology, 212p.

Lin C.M., Chang T.M., Huang Y.C., Chiang H.J., Kuo C.H., Wen K.L., 2009. Shallow S-Wave Velocity Structures in the Western Coastal Plain of Taiwan. Terr. Atmos. Ocean. Sci., 20(2), 299-308.

Lin C.M., Wen K.L., Huo C.H., Lin C.Y., 2014. S-wave velocity model of Taipei basin. The 5th Asia Conference on Earthquake Engineering October 16-18.

Miller R.D., Xia J., Park C.B., Ivanov J., Williams E., 1999. SEG Annual Meeting, Houston, Texas.

Molnar S., Cassidy J.F., Castellaro S., Cornou C., Crow H., Hunter J.A., Matsushima S., Sánchez-Sesma F.J., Yong A., 2018. Application of Microtremor Horizontal-to-Vertical Spectral Ratio (MHVSR) Analysis for Site Characterization: State of the Art. Surv Geophys., 39, 613-631.

Nakamura Y., 1989. A Method for dynamic characteristics estimation of subsurface using microtremor on the ground surface. Quarterly Report of RTRI, 30(1), 25-33.

Ngal N.L., Pramumijoyo S., Satyarno I., Brotopuspito K.S., Kiyono J., Hartantyo E., 2019. Multi-channel analysis of surface wave method for geotechnical site characterization in Yogyakarta, Indonesia. E3S Web of Conferences ICST 2018, 76, 03006.

Nguyen Duc Dai (project manager), 1996. Final report of geological survey for Hanoi city. Department of Geology, 178p (in Vietnamese).

Nguyen Dinh Thong, Nguyen Ba Binh, Doan Thi Du, Trinh Thi Thuy Hang, Le Thi Han, Nguyen Thi Thanh Huong, Dang Ngoc Thuy, Pham Duy Trinh, 2012. Final report on investigation and assessment of underground water in the Neogen layer for Hanoi city (in Vietnamese).

Nguyen Dinh Xuyen (project manager), 1994. Completion of the microzoning map of Hanoi city at 1:25,000 scale. Final report of the City project, Institute of Geophysics (in Vietnamese).

Nguyen Hong Phuong (project manager) 2014. Site Effects estimation and urban seismic risk assessment for Hanoi city, Final report of national project, Institute of Geophysics, Hanoi (in Vietnamese).

Nguyen Manh Tuan, 1990. Seismic microzoning in Hanoi city. Science and Technics Publishing House, 106p (in Vietnamese).

Nguyen Tien Hung, Kuo-Liang Wen, 2011. Seismic microzoning map of Hanoi city on the basis of microtremor motion observations. Sciences of the Earth, 33(2), 175-184 (in Vietnamese).

Parolai S., Bormann P., Milkereit C., 2002. New relationships between V_S, thickness of sediments, and resonance frequency calculated by the H/V ratio of seismic noise for the Cologne area (Germany). Bulletin of the Seismological Society of America, 92(1), 2521-2527.

Pham The Truyen, Nguyen Hong Phuong, 2019. Probabilistic seismic hazard assessment for Hanoi city. Science of the Earth, 41(4), 321-338.

Phan Trong Trinh, Ngo Van Liem, Nguyen Van Huong, Hoang Quang Vinh, Bui Van Thom, Bui Thi Thao, Mai Thanh Tan, Nguyen Hoang, 2012. Late Quaternary tectonics and seismotectonics along the Red River fault zone, North Vietnam. Earth-Science Reviews, 114, 224-235.

Phan Trong Trinh, Hoang Quang Vinh, Nguyen Van Huong, Ngo Van Liem, 2013. Active fault segmentation and seismic hazard in Hoa-Binh reservoir, Vietnam, Cent. Eur. J. Geosci., 5(2), 223-235.

Satoh T., Kawase H., Iwata T., Higashi S., Sato T., Irikura K., Huang H.C., 2001. S-Wave Velocity Structure of the Taichung Basin, Taiwan, Estimated from Array and Single-Station Records of Microtremors. Bulletin of the Seismological Society of America, 91(5), 1267-1282.

Seht, Wohlenberg, 1999. Microtremor Measurements Used to Map Thickness of Soft Sediments. Bulletin of the Seismological Society of America, 89(1), 250-259.

Singh S.K., Mena E., Castro R., 1988. Some aspects of source characteristics of the 19 September Michoacan earthquake and ground amplification in and near Mexico City from strong ground motions data. Bull. Seism. Soc. Am., 78(2), 451-457.

Tokeshi J.C., Karkee M.B., Sugimura Y., 2006. Reliability of rayleigh wave dispersion curve obtained from f-k spectral analysis of microtremor array measurement. Soil Dynamics and Earthquake Engineering, 26, 163-174.

Tran Thi My Thanh, Nguyen Anh Duong, Nguyen Le Minh, Nguyen Thanh Tung, Pham Quang Hung, 2006. Experimental application of SPAC method in processing microseismic data in Vietnam. Journal of Geology, 297, 57-64 (in Vietnamese).

Tulandhar R., Cuong N.N.H., Yamazaki F., 2004. Seismic microzonation of Hanoi, Vietnam using microtremor observations. 13th World Conference on Earthquake Engineering, Vancouver, B.C., Canada, August1-6, 2539.

Tün M., Pekkan E., 2022. Sunay Mutlu The depth of alluvial sediments and subsurface profiling along the Eskişehir Basin in Central Turkey using microtremor observations. Bulletin of Engineering Geology and the Environment, 81, 169.

Vu Nhat Thang, Chau Van Quynh, Dang Van Doi, La Van Xuan, Ngo Quang Toan, Nguyen Cong Luong, Nguyen Van Can, Nguyen Van Dan, Pham Van Man, Phan Hong Dan, 2003. Geology and minerals resources of Hanoi. General Department of Geology and Minerals of Vietnam, 290p (in Vietnamese).